SRTTU
Journal of Computational and Applied Research in Mechanical Engineering
jcarme.sru.ac.ir
JCARME
ISSN: 2228-7922

Research paper

Investigation of natural convection heat transfer of MHD hybrid nanofluid in a triangular enclosure

Ali Akbar Rashidi and Ehsan Kianpour*

Department of Mechanical Engineering, Faculty of Engineering, Najafabad Branch, Islamic Azad University, Najafabad, Isfahan, Iran

Article info:

Article history:

Received: 30/12/2017
Revised: 02/01/2019
Accepted: 05/01/2019
Online: 08/01/2019

Keywords:

Hybrid nanofluid,
Natural convection,
Heat transfer,
Magnetic field.

***Corresponding author:**
ekianpour@pmc.iaun.ac.ir

Abstract

Natural convection heat transfer is studied numerically in a triangular enclosure. The enclosure is isosceles right triangle and its bottom wall is hot, the hypotenuse is cold and the other wall is adiabatic. Also, a vertical magnetic field is applied in the enclosure; and there is hybrid nanofluid inside the enclosure. This study is conducted for Rayleigh numbers of 103-105, the Hartmann numbers between 0-80, and the volume fraction of nanofluid is between 0-2 percent. Based on the obtained results, as the Hartmann number augments, the temperature of the center of the enclosure decreases due to weakening of the heat transfer flow by increasing the magnetic field forces. In addition, as the Hartmann number augments, the streamlines approach to the walls because the horizontal momentum forces decrease when the Hartmann number increases. Furthermore, by increasing the density of nanoparticles, the heat transfer rate increases, and as a result, heat transfer builds up. Finally, heat transfer improves when the hybrid-nanofluid is employed rather than ordinary nanofluid.

1. Introduction

As far as conventional fluids have low thermal conductivity, they limited the heat transfer rate in industry. Therefore, for enhancing the heat transfer, using nanofluid, dilute suspensions of nanoparticles in liquids can be introduced as a practical approach. Quite a few studies have been conducted and devoted to extract empirical models for nanofluids and using these models in practical examples in nature and industry [1-10].

Aghaei et al. [2] considered a trapezoidal enclosure and by employing the the finite volume method they scrutinized the velocity field and temperature distribution in such enclosure. The working fluid was water accompanied by Cu nanoparticles which leads to considering the magnetic field in the enclosure. They found out that volume fraction of nanoparticles has a direct effects on increasing the Nusselt number and entropy generation, whilst this behaviour is reversed for the Hartmann number; and as the Hartmann number augments, both of the aforementioned numbers would reduce. In another numerical simulation, Abbaszadeh et al. [1] employed KKL model for CuO-water nanofluid in order to consider the effects of the Brownian motions of nanoparticles. The algorithm they used was SIMPLER with the aim of Finite Volume Method in order to solve the set of Naveir-Stokes equations (for obtaining the flow field) and energy equation (for measuring the temperature field). As far as their problem geometry was a parallel plate microchannel, they considered the slip boundary condition in their walls, and the magnetic field effects is reflected in their study by the Hartmann number. They demonstarted that by increasing the fluid inertia force, the nanoparticles density and magnetic field effect will cause an increment in total entropy generation and the anerage Nusselt number. In another study, Ababaei et al. [11] with the aim of finding the optimum location of the impediments for enhancing the heat transfer rate inside a microchannel employed the FVM numerical method. In their study, the working nanofluid was Al_2O_3-water whose characteristics have been obtaind by Khanafer and Vafaei's model [12] which is a variable properties model. Again, they endorsed that increasing the momentum of the nanofluid results in the enhancment of the heat transfer inside the microchannel. Therefore, it would be benefitial if we keep the Reynolds number high enough to augment the Nusselt number. With the same reason, the total entropy generation will increase. Very recently, Hashim et al. [13] studied the heat transfer enhancement of Al_2O_3-water inside a wavy cavity using Finite Element numerical method. They did partial heating from the bottom wall whilst the side wavy walls were isothermal and the top wall was insulated. They used different types of oscilations for the wavy walls to find he optimum case in terms of increasing the Nusselt number. They showed that nanoparticles caused an increase in the heat transfer rate inside the cavity.

Even though adding nanoparticles to the base fluid can enhance the heat transfer rate in many applications, the desire for improving the heat transfer leads to introducing a new type of nanofluid which is called "hybrid nanofluid" [14, 15]. Actually, the hybrid naniofluid is a composite of single nanoparticle and we want to show how this composition will affect the heat transfer rate in industry and nature. Suresh et al. [16] employed the hybrid nanofluid concept and used Al_2O_3–Cu/water hybrid nanofluid. Their working geometry was a circular tube, which is uniformly heated in a laminar flow regime. They showed that the heat transfer rate will increase by 13.56% in Re=1730 when they applied hybrid nanofluid compared to pure water. In another numerical investigation, Moghadassi et al. [17] considered the forced convection heat transfer of Al_2O_3–Cu/water hybrid nanofluid to compare the heat transfer rate and examine if using hybrid nanofluid improves the heat transfer rate or not. For this purpose, they also calculated the average Nusselt number of pure water and Al_2O_3-water nanofluid. They demonstrated that the heat transfer rate of hybrid nanofluid is by far higher than other cases.

By a closer look at the literature, we can realize that little attention has been paid to using hybrid nanofluid in cavities and enclosures. Thus, in the current study, the natural convection of Al_2O_3-Cu/water hybrid nanofluid is examined in a right-angled enclosure. Moreover, there is a magnetic field in flow field and the effects of magnetic field is also investigated. The governing equations are solved using the Finite Volume (FV) method for the Rayleigh numbers of 10^3, 10^4, and 10^5, the Hartmann numbers of 0-40-80, and the volume fraction of nanoparticles of 0-2 percent.

2. Mathematical formulation

The geometrical configuration of the microchannel is depicted in Fig. 1. The vertical wall is insulated, the horizontal wall is hot, and the hypotenuse is cold. Also, there is an upward magnetic field in the enclosure and the enclosure is filled with Al_2O_3-Cu/water hybrid nanofluid. The nanofluid is considered to be Newtonian and incompressible. The effect of density variation is neglected except for the buoyancy term, where it is approximated by the well-known Boussinesq correlation. The viscous dissipation effect is

neglected as well. The working nanoparticles are Al_2O_3 and Cu nanoparticles (see Table 1).
The range of nanoparticles volume fraction (90% Al_2O_3 and 10% Cu by volume) is between 0% and 2%. The hybrid nanofluid density [18], heat capacity [19] and electrical conductivity [20], viscosity and thermal conductivity [14] are given by the following relations respectively:

$$\rho_{nf} = (1-\varphi)\rho_f + \varphi\rho_s \quad (1)$$

$$\rho_{nf} c_{p_{nf}} = (1-\varphi)c_{p_f}\rho_f + \varphi c_{p_s}\rho_s \quad (2)$$

$$\frac{\sigma_{nf}}{\sigma_f} = 1 + \frac{3(\frac{\sigma_p}{\sigma_f}-1)\varphi}{(\frac{\sigma_p}{\sigma_f}+2)-(\frac{\sigma_p}{\sigma_f}-1)\varphi} \quad (3)$$

$$\frac{\mu_{nf}}{\mu_f} = -1283\varphi^2 + 8431\varphi + 0.9454 \quad (4)$$

$$\frac{k_{nf}}{k_f} = -151.5\varphi^2 + 8.916\varphi + 1.004 \quad (5)$$

It is worth mentioning that the Eqs. (4 and 5) are derived from an experimental model [14] which are correlated by Mollamahdi et al. [21].
The Naiver-Stokes equations accompanied by energy equations for laminar and natural convection of the hybrid nanofluid flow are given by:

$$\frac{\partial}{\partial x}(u) + \frac{\partial}{\partial y}(v) = 0 \quad (6)$$

$$\frac{\partial}{\partial x}(uu) + \frac{\partial}{\partial y}(vu) = \frac{1}{\rho_{nf}}\left[-\frac{\partial p}{\partial x} + \frac{\partial}{\partial x}\left(\mu_{nf}\frac{\partial u}{\partial x}\right) + \frac{\partial}{\partial y}\left(\mu_{nf}\frac{\partial u}{\partial y}\right) + \sigma_{nf} B_0^2 u\right] \quad (7)$$

$$\frac{\partial}{\partial x}(uv) + \frac{\partial}{\partial y}(vv) = \frac{1}{\rho_{nf}}\left[-\frac{\partial p}{\partial y} + \frac{\partial}{\partial x}\left(\mu_{nf}\frac{\partial v}{\partial x}\right) + \frac{\partial}{\partial y}\left(\mu_{nf}\frac{\partial v}{\partial y}\right) + (\rho\beta)_{nf}\, g\,(T-T_c)\right] \quad (8)$$

$$\frac{\partial}{\partial x}(uT) + \frac{\partial}{\partial y}(vT) = \frac{1}{(\rho c_p)_{nf}}\left[\frac{\partial}{\partial x}\left(k_{nf}\frac{\partial T}{\partial x}\right) + \frac{\partial}{\partial y}\left(k_{nf}\frac{\partial T}{\partial y}\right)\right] \quad (9)$$

u and v are representative of velocity fields in this 2D environment in x and y directions respectively. Dynamic viscosity is μ, electrical conductivity is σ, fluid density is ρ, c_p is heat capacity at constant pressure, and k is the thermal conductivity.
The dimensionless parameters for casting the mentioned equations into the non-dimensional form is as follows:

$$(X,Y) = \frac{(x,y)}{L}, \quad (U,V) = (u,v)\frac{L}{\alpha_{bf}},$$
$$P = \frac{pL^2}{\rho_{nf}\alpha_{bf}^2}, \quad \theta = \frac{T-T_c}{\Delta T} \quad (10)$$
$$\mathrm{Pr} = \frac{\nu_{bf}}{\alpha_{bf}}; \quad \mathrm{Ha} = B_0 L\sqrt{\frac{\sigma_{bf}}{\mu_{bf}}};$$
$$\mathrm{Ra} = \frac{g\beta_{bf}\Delta T L^3}{\nu_{bf}\alpha_{bf}}$$

where $\Delta T = T_h - T_c$. Hence, the representation of the non-dimensionalized equations are:

$$\frac{\partial U}{\partial X} + \frac{\partial V}{\partial Y} = 0 \quad (11)$$

$$\frac{\partial}{\partial X}(UU) + \frac{\partial}{\partial Y}(VU) = -\frac{\partial P}{\partial X} + \frac{\rho_{bf}}{\rho_{nf}\mu_{bf}}\mathrm{Pr}\left[\frac{\partial}{\partial X}\left(\mu_{nf}\frac{\partial U}{\partial X}\right) + \frac{\partial}{\partial Y}\left(\mu_{nf}\frac{\partial U}{\partial Y}\right)\right] - \frac{\sigma_{nf}}{\sigma_{bf}}\frac{\rho_{bf}}{\rho_{nf}}\mathrm{Ha}^2\,\mathrm{Pr}\,U \quad (12)$$

$$\frac{\partial}{\partial X}(UV) + \frac{\partial}{\partial Y}(VV) = -\frac{\partial P}{\partial Y} + \frac{\rho_{bf}}{\rho_{nf}\mu_{bf}}\mathrm{Pr}\left[\frac{\partial}{\partial X}\left(\mu_{nf}\frac{\partial V}{\partial X}\right) + \frac{\partial}{\partial Y}\left(\mu_{nf}\frac{\partial V}{\partial Y}\right)\right] + \frac{(\rho\beta)_{nf}}{\rho_{nf}\beta_{bf}}\mathrm{Ra}\,\mathrm{Pr}\,\theta \quad (13)$$

$$\frac{\partial}{\partial X}(U\theta) + \frac{\partial}{\partial Y}(V\theta) = \frac{(\rho c_p)_{bf}}{k_{bf}(\rho c_p)_{nf}}\left[\frac{\partial}{\partial X}\left(k_{nf}\frac{\partial \theta}{\partial X}\right) + \frac{\partial}{\partial Y}\left(k_{nf}\frac{\partial \theta}{\partial Y}\right)\right] \quad (14)$$

The local Nusselt number is obtained from the following relation:

$$\mathrm{Nu} = -\left(\frac{k_{nf}}{k_{bf}}\right)\frac{\partial\theta}{\partial n}\bigg|_{hot\ \ walls} \quad (15)$$

where n is the normal direction from the hot obstacle. Thus, the average Nusselt number can be calculated by integrating from Eq. (15) along the hot surface:

$$\mathrm{Nu}_{av} = \frac{\int_L \mathrm{Nu}\,dL}{\int_L dL} \quad (16)$$

where L is the length of the hot surface.

3. Numerical implementation

The numerical method which has been used in this study is called SIMPLER algorithm and Finite Volume Method (FVM). In this method, initially, a fine grid should be defined over the problem domain and around each node, a volume should be considered. Then, after integrating and discretizing equations, the PDEs will be simplified. Then, with the help of line-by-line TDMA solver, the discretized equations are solved.

3.1. Mesh independence test

If the results of a numerical simulation depends on the grids size, the accuracy of the results will be overshadowed. Thus, we run a grid independency test to ensure the accuracy of the results for natural-convection flow of Al_2O_3-Cu/water hybrid nanofluid in the right-angled triangle enclosure at $\mathrm{Ha}=40$, $\mathrm{Ra}=10^4$ and $\phi=0.02$. The obtained average Nusselt number for different girds is presented in Table 2. As evidenced by this table, 5101 is an appropriate grid size which guarantees proper numerical modeling.

3.2. Computer program verification

In order to ascertain the validity of the computer used in this study, some cases of Kaluri et al. [22] and Yesiloz and Aydin [23] studies are modeled with the current program and their results are evaluated in Fig. 2 and Table 3. In Fig. 2 the streamlines and isotherms are depicted; and in Table 3 the stream function difference is compared. As can be observed, an excellent conformance exists between our simulation and those of Kaluri et al. [22] and Yesiloz and Aydin [23], which certifies modeling results accuracy.

4. Results and discussion

Fluid field and heat transfer of MHD Al_2O_3-Cu/water hybrid nanofluid are investigated in a right-angled triangle. The effect of different parameters such as Rayleigh number, magnetic field intensity and nanoparticles density on average Nusselt number is evaluated. This study was conducted for the Rayleigh numbers of 10^3, 10^4, and 10^5, the Hartmann numbers of 0-40-80, and the volume fraction of nanoparticles of 0-2 percent.

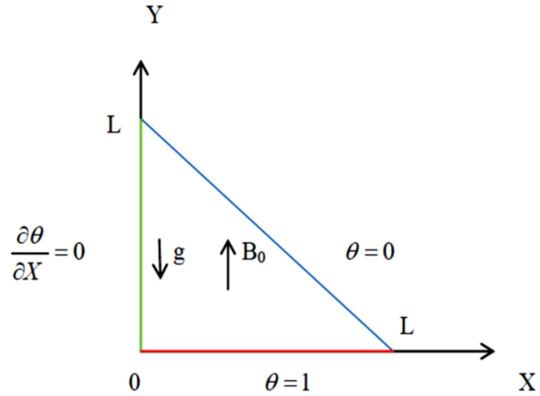

Fig. 1. Schematic of the problem.

Table 1. Thermo-physical properties of Al_2O_3 and Cu nanoparticles; and water as a base fluid [1, 18].

	$\rho(kg/m^3)$	c_p (j/kg K)	K (W/m K)	$\sigma(\Omega.m)^{-1}$	Pr
Al_2O_3	3970	765	25	1×10^{-10}	-
Cu	3954	383	400	5.96×10^{7}	-
Pure Water	997.1	4179	0.613	0.05	6.2

Table 2. Nu_{av} in different grid size at $\mathrm{Ha}=40$ and $\mathrm{Ra}=10^4$ $\phi=0.02$.

Number of control volume	Nu_{av}	Relative (%) error
1301	8.87	-
5101	9.01	1.58
11401	9.02	0.11

Table 3. Comparisons of stream function difference between present study and Yesiloz and Aydin [23].

Rayleigh number		10^6	10^5	10^4	10^3
Yesiloz and Aydin [23]	$\Delta\Psi$	32.92	12.12	2.62	0.215
Present study	$\Delta\Psi$	33.08	12.02	2.60	0.213
Relative (%) difference		0.48	0.82	0.76	0.93

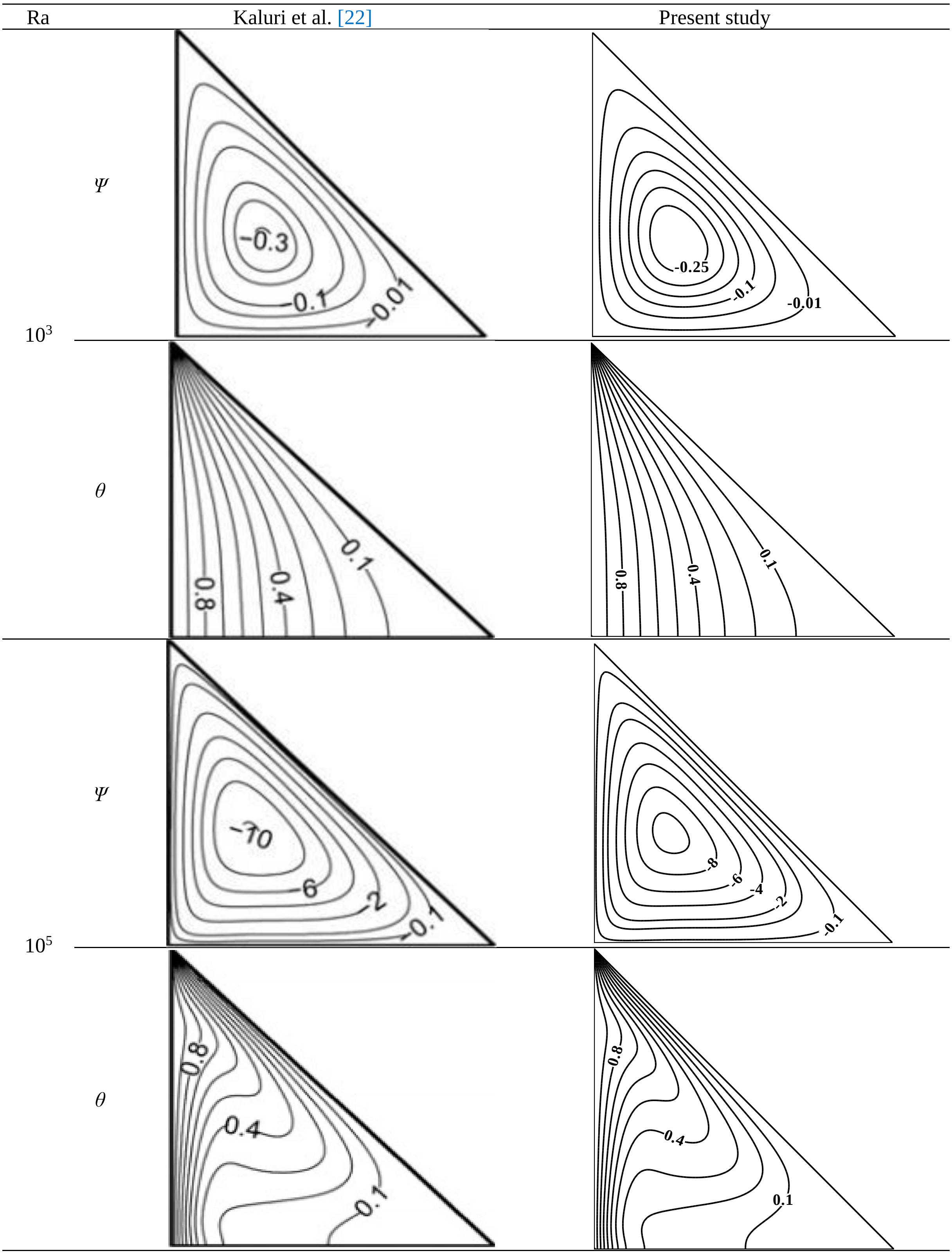

Fig. 2. Comparisons of the streamlines and isotherms in the present study and Kaluri et al. [22] in different Rayleigh numbers.

4.1. Streamlines and isotherms

The variations of the streamlines for Al_2O_3-Cu/water hybrid nanofluid and pure water in different Rayleigh and Hartmann numbers are displayed in Fig. 3. Generally, in Rayleigh numbers of 10^3 and 10^4 there is a clockwise vortex; however, in Rayleigh number of 10^5, by increasing the buoyancy forces and their dominance over the viscosity forces, in some cases a counter clockwise vortex is formed. In this Rayleigh number and in Ha=40, there are two vortices for the base fluid and one vortex for hybrid nanofluid. The reason of this phenomenon is that by adding nanoparticles, the viscosity forces augment and they do not allow a second vortex to be created. Generally, as the Hartmann number augments, the streamlines approach to the walls since the horizontal momentum forces decrease when the Hartmann number increase.

Fig. 4 indicates the variations of the isotherms for Al_2O_3-Cu/water hybrid nanofluid and pure water in different Rayleigh and Hartmann numbers. In Rayleigh numbers of 10^3 and 10^4, the isotherms are stratified since the conduction heat transfer regime is the dominant regime in the enclosure. Although it is definitely true that the Rayleigh numbers of 10^3 and 10^4 have one order difference, both of them are in the range of the conduction heat transfer regime physically. Thus, the obtained results for both of them are analogous. Furthermore, by increasing the Hartmann number, the difference between isotherms becomes lower and they coincide with each other more and more since the momentum reduces as the Hartmann number increases. Moreover, in Ra=10^4 and Ha=0 and also in Ra=10^5 and Ha=0 and 40 the stratified form of isotherms is disturbed for the pure water and these lines approach the cold wall. Hence, in these cases, the temperature gradients on the cold walls build up and as a result, the heat transfer augments. Another astonishing point is that although in Ra=10^5 the buoyancy forces are strengthen and the convection regime is the dominant regime, in Ha=80 there is a similar regime (conduction regime) like the aforementioned cases as far as the horizontal momentum forces reduce by increasing the Hartmann number.

Variations of the dimensionless temperature in the horizontal section of the enclosure in different Hartmann numbers are displayed in Fig. 5. As can be seen in this figure, by increasing the Hartmann number, the temperature of the central section in the enclosure reduces since the flow weakens by increasing the Hartmann number.

Variations of the horizontal components of the dimensionless velocity in the vertical section of the enclosure in different Hartmann numbers are depicted in Fig. 6 In three Hartmann numbers a clockwise vortex is seen in the enclosure. Moreover, by increasing the Hartmann number, the momentum forces decrease.

Fig. 7 shows the variations of the vertical components of the dimensionless velocity in the horizontal section of the enclosure in different Hartmann numbers. Similar to Fig. 6, a clockwise vortex is observed in the enclosure that by increasing the Hartmann number the variation range of this vortex decreases.

The variation of the dimensionless temperature in the horizontal section of the enclosure in different volume fractions of nanoparticles is displayed in Fig. 8. Generally, as the φ augments, the dimensionless temperature in the central section reduces.

Variation of the horizontal components of the dimensionless velocity in the vertical section of the enclosure in different volume fractions of nanoparticles is shown in Fig. 9. As can be seen in this figure, by increasing the volume fraction of nanoparticles, the range of the horizontal velocity decreases since the dynamic viscosity of the nanofluid compared to the base fluid augments that results in reducing the velocity gradient all over the enclosure.

Fig. 10 reveals the variation of the vertical components of the dimensionless velocity in the horizontal section of the enclosure in different volume fractions of nanoparticles. Like the foregoing figure, as the volume fraction of nanoparticles increases, the velocity gradient decreases all over the enclosure.

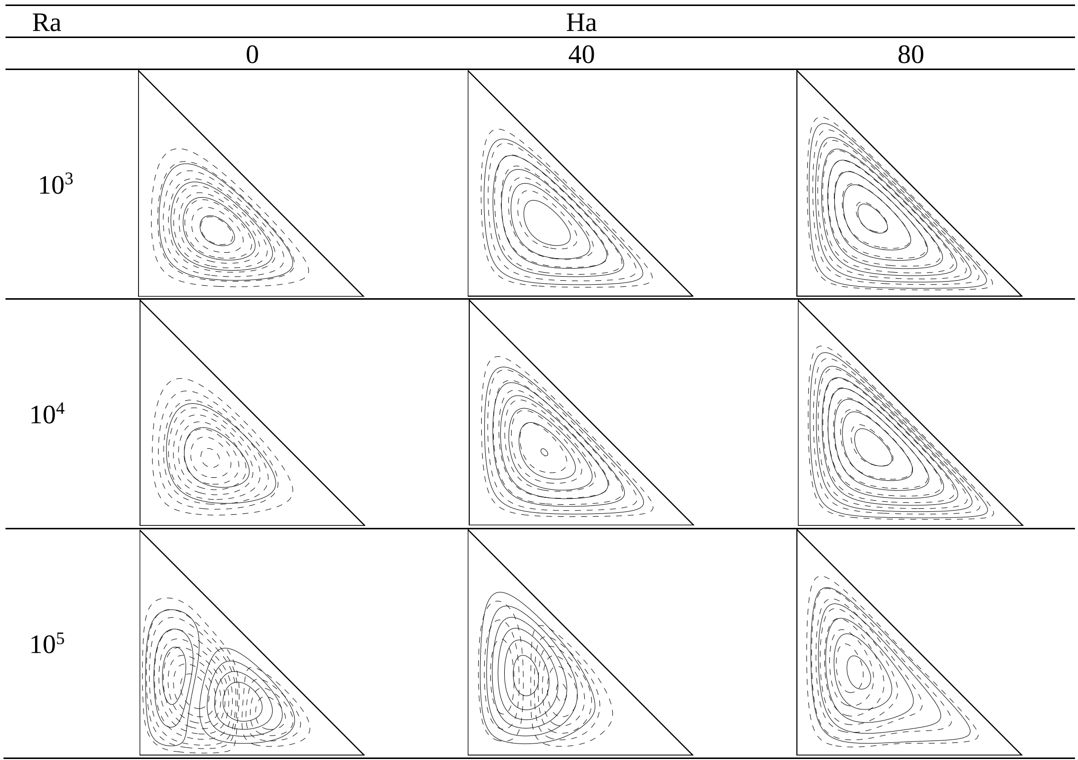

Fig. 3. Variations of the streamlines for Al_2O_3-Cu/water hybrid nanofluid (—) and pure water (- -).

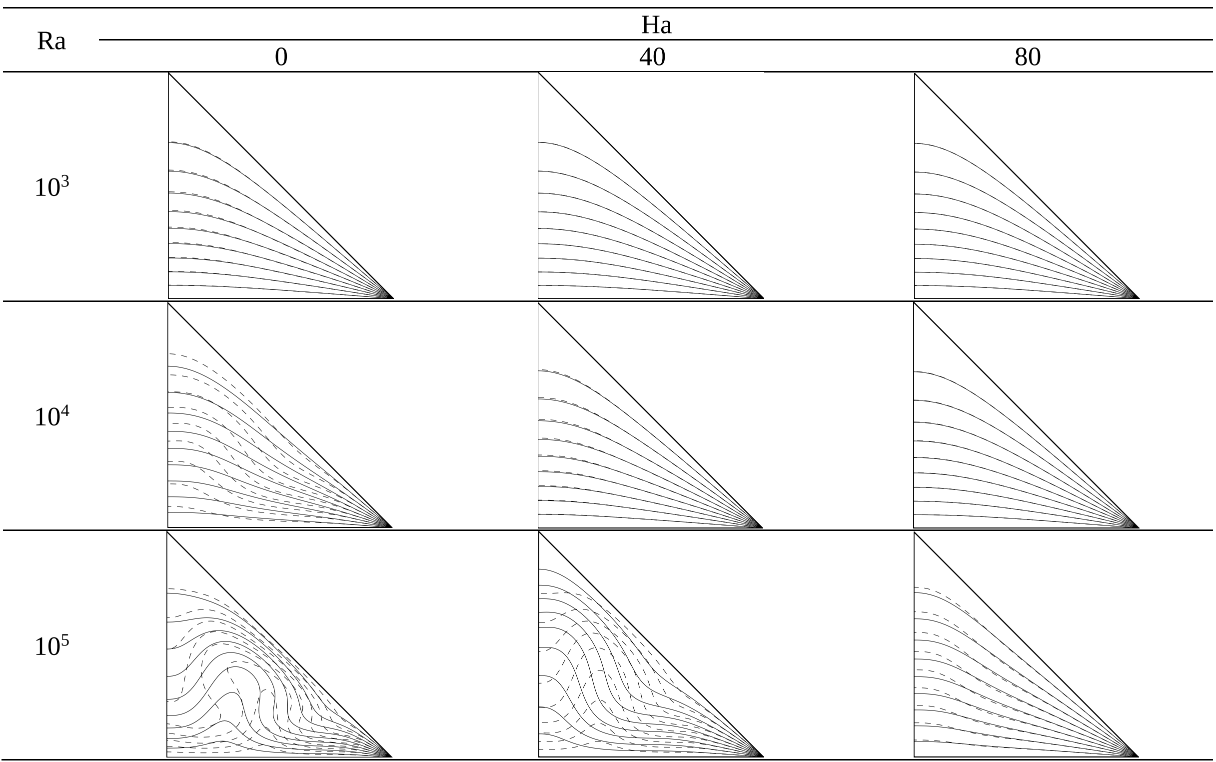

Fig. 4. Variations of the isotherms for pure water (- -) and Al_2O_3-Cu/water hybrid nanofluid (—).

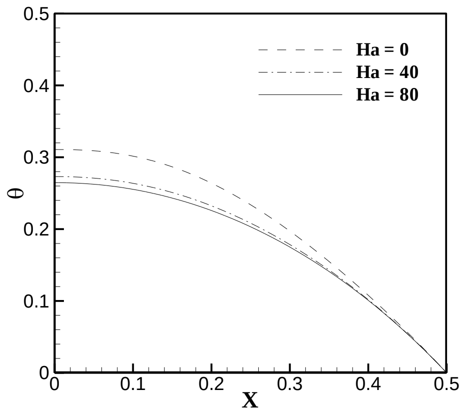

Fig. 5. Variations of the dimensionless temperature in the horizontal section of the enclosure in different Ha and in Ra=10^4 and $\varphi = 0.02$.

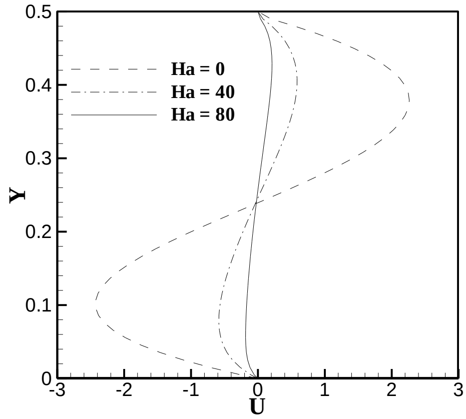

Fig. 6. Variations of the horizontal components of the dimensionless velocity in the vertical section of the enclosure in different Ha and in Ra=10^4 and $\varphi = 0.02$.

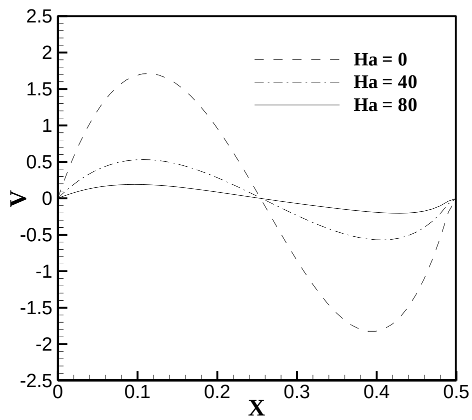

Fig. 7. Variations of the vertical components of the dimensionless velocity in the horizontal section of the enclosure in different Ha and in Ra=10^4 and $\varphi = 0.02$.

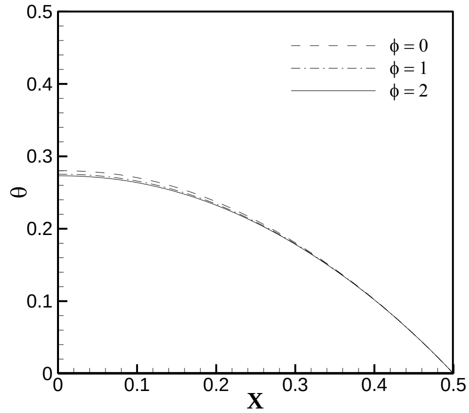

Fig. 8. Variation of the dimensionless temperature in the horizontal section of the enclosure in different φ and in Ra=10^4 and Ha=40.

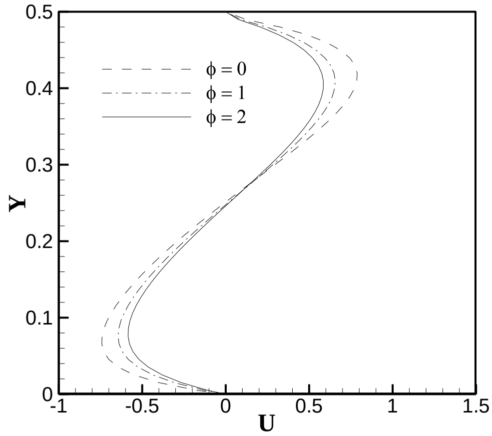

Fig. 9. Variation of the horizontal components of the dimensionless velocity in the vertical section of the enclosure in different φ in Ra=10^4 and Ha=40.

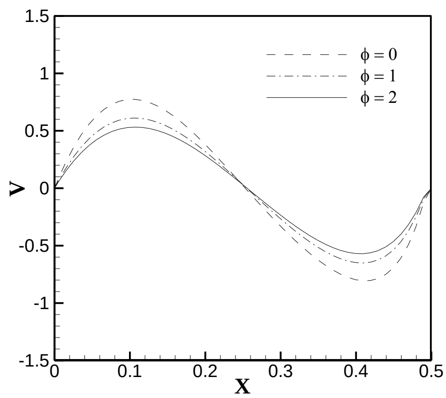

Fig. 10. Variation of the vertical components of the dimensionless velocity in the horizontal section of the enclosure in different φ and in Ra=10^4 and Ha=40.

4.2. Heat transfer rate

The variations of the Nu_{av} via φ in different Ra is shown in Fig. 11. The results for the Ra=10^3 and 10^4 are the same since the heat transfer regimes are the same, but in Ra=10^5 in all the cases the Nu_{av} is more than other cases since the buoyancy forces become stronger and the convection heat transfer becomes dominant in the enclosure. Moreover, by increasing the φ the heat transfer inceases.

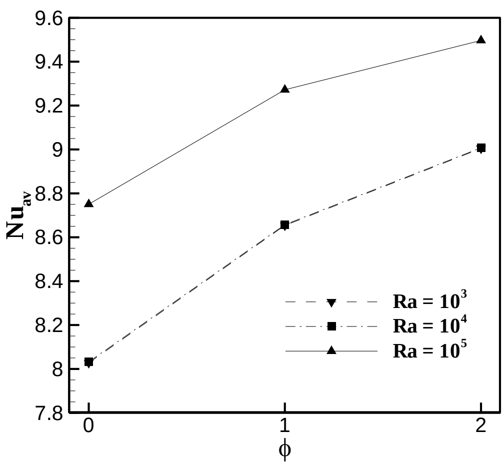

Fig. 11. Variations of the Nu_{av} via the φ in different Ra and in Ha=40.

The comparisons of the Nu_{av} on the hot wall between hybrid nanofluid and ordinary water-Al_2O_3 nanofluid is indicated in Table 4. As it is obvious in this figure, the hybrid nanofluid has a better thermal characteristic in comparison to ordinary nanofluid. It is noteworthy that for modeling the ordinary nanofluid, the Brinkman [24] and Maxwcll-Garnctt [25] models have been employed to calculate the viscosity and thermal conductivity of the nanofluid.

Table 4. The comparisons of the Nu_{av} on the hot wall between hybrid nanofluid and ordinary water-Al_2O_3 nanofluid.

Increment(%)	nanofluid		(%) ϕ
	Al_2O_3-Cu/water	Water-Al_2O_3	
0	8.24	8.24	0
3.08	8.70	8.44	1
4.51	9.03	8.64	2

5. Conclusions

Finite Volume numerical method has been employed in the current study to simulate the effects of using Al_2O_3-Cu/water hybrid nanofluid in a right-angled triangle on improving heat transfer rate. This study was conducted for the Ra of 10^3, 10^4, and 10^5, the Ha of 0-40-80, and the φ of 0-2 percent. The results show that:

- As the Hartmann number augments, the streamlines approach the walls since the horizontal momentum forces decrease when the Hartmann number increases.
- As the φ augments, the dimensionless temperature in the central section reduces.
- In Ra=10^5, the Nu_{av} is more than other Rayleigh numbers since the buoyancy forces become stronger and the convection heat transfer becomes dominant in the enclosure.
- The hybrid nanofluid has a better thermal characteristic in comparison to ordinary nanofluid.

Reference

[1] M. Abbaszadeh, A. Ababaei, A. A. A. Arani, and A. A. Sharifabadi, "MHD forced convection and entropy generation of CuO-water nanofluid in a microchannel considering slip velocity and temperature jump", *J. Braz. Soc. Mech. Sci. Eng.* , Vol. 39, No. 3, pp. 775-790, (2017).

[2] A. Aghaei, H. Khorasanizadeh, G. A. Sheikhzadeh, and M. Abbaszadeh, "Numerical study of magnetic field on mixed convection and entropy generation of nanofluid in a trapezoidal enclosure," *J. Magn. Magn. Mater.*, Vol. 403, pp. 133-145, (2016).

[3] A. R. Rahmati, A. R. Roknabadi, and M. Abbaszadeh, "Numerical simulation of mixed convection heat transfer of nanofluid in a double lid-driven cavity using lattice Boltzmann method," *Alexandria. Eng. J.*, Vol. 55, No. 4, pp. 3101-3114, (2016).

[4] M. Mollamahdi, M. Abbaszadeh, and G. A. Sheikhzadeh, "Flow field and heat transfer in a channel with a permeable

wall filled with Al2O3-Cu/water micropolar hybrid nanofluid, effects of chemical reaction and magnetic field," *J. Heat Mass Transfer. (JHMTR)*, Vol. 3, No. 2, pp. 101-114, (2016).

[5] G. Sheikhzadeh, H. Ghasemi, and M. Abbaszadeh, "Investigation of natural convection boundary layer heat and mass transfer of MHD water-AL2O3 nanofluid in a porous medium," *Int. J. Nano Stud. Tech. (IJNST)*, Vol. 5, No. 2, pp. 110-122, (2016).

[6] G. Sheikhzadeh, A. Aghaei, H. Ehteram, and M. Abbaszadeh, "Analytical study of parameters affecting entropy generation of nanofluid turbulent flow in channel and micro-channel," *Therm. Sci.*, (2016).

[7] A. Abbasian Arani, J. Amani, and M. Hemmat Esfeh, "Numerical simulation of mixed convection flows in a square double lid-driven cavity partially heated using nanofluid," *J. Nano-Struct.*, Vol. 2, No. 3, pp. 301-311, (2012).

[8] A. Ababaei, M. Abbaszadeh, A. Arefmanesh, and A. J. Chamkha, "Numerical simulation of double-diffusive mixed convection and entropy generation in a lid-driven trapezoidal enclosure with a heat source", *Numer. Heat Trans. A-Appl.* , Vol. 73, No. 10, pp. 1-19, (2018).

[9] A. Abbasian Arani, M. Abbaszadeh, and A. J. T. P. N. M. S. Ardeshiri, "Mixed convection fluid flow and heat transfer and optimal distribution of discrete heat sources location in a cavity filled with nanofluid", *Chall. Nano Micro Scale Sci. Tech.*, Vol. 5, No. 1, pp. 30-43, (2016).

[10] A. Ababaei, M. Abbaszadeh, and A. A. Abbasian Arani, "Determining the optimum arrangement of micromixers in a microchannel filled with CuO-water nanofluid via minimizing entropy generation," *Defect Diffus. Forum*, Vol. 378, pp. 39-58: Trans Tech Publ, (2017).

[11] A. Ababaei and M. J. G. J. o. N. Abbaszadeh, "Second Law Analyses of Forced Convection of Low-Reynolds-Number Slip Flow of Nanofluid Inside a Microchannel with Square Impediments", *Glob. J. Nano-med.*, Vol. 1, No. 4, (2017).

[12] K. Khanafer, K. J. I. j. o. h. Vafai, and m. transfer, "A critical synthesis of thermophysical characteristics of nanofluids", *Int. J. Heat Mass Transfer*, Vol. 54, No. 19-20, pp. 4410-4428, (2011).

[13] I. Hashim, A. Alsabery, M. Sheremet, and A. J. A. P. T. Chamkha, "Numerical investigation of natural convection of Al2O3-water nanofluid in a wavy cavity with conductive inner block using Buongiorno's two-phase model", *Adv. Powder Tech.* Vol. 30, No. 2, pp. 399-414, (2018).

[14] S. Suresh, K. Venkitaraj, P. Selvakumar, and M. Chandrasekar, "Synthesis of Al 2 O 3–Cu/water hybrid nanofluids using two step method and its thermo physical properties," *Colloids Surf. A Physicochem. Eng. Asp.*, Vol. 388, No. 1, pp. 41-48, (2011).

[15] M. Mollamahdi, M. Abbaszadeh, and G. A. J. S. I. Sheikhzadeh, "Analytical study of Al2O3-Cu/water micropolar hybrid nanofluid in a porous channel with expanding/contracting walls in the presence of magnetic field", *Int. J. Sci. Tech.*, Vol. 25, No. 1, pp. 208-220, (2018).

[16] S. Suresh, K. Venkitaraj, P. Selvakumar, and M. Chandrasekar, "Effect of Al 2 O 3–Cu/water hybrid nanofluid in heat transfer," *Exp. Therm. Fluid Sci.*, Vol. 38, pp. 54-60, (2012).

[17] A. Moghadassi, E. Ghomi, and F. Parvizian, "A numerical study of water based Al 2 O 3 and Al 2 O 3–Cu hybrid nanofluid effect on forced convective heat transfer," *Int. J. Therm. Sci.*, Vol. 92, pp. 50-57, (2015).

[18] S. K. Das, S. U. Choi, W. Yu, and T. Pradeep, *Nanofluids: science and technology*. John Wiley & Sons, (2007).

[19] Y. Xuan and W. Roetzel, "Conceptions for heat transfer correlation of nanofluids," *Int. J. Heat Mass Transfer.*, Vol. 43, No. 19, pp. 3701-3707, (2000).

[20] A. El Jery, N. Hidouri, M. Magherbi, and A. B. Brahim, "Effect of an external oriented magnetic field on entropy

generation in natural convection," *Entropy*, Vol. 12, No. 6, pp. 1391-1417, (2010).

[21] M. Mollamahdi, M. Abbaszadeh, and G. A. Sheikhzadeh, "Flow field and heat transfer in a channel with a permeable wall filled with Al2O3-Cu/water micropolar hybrid nanofluid, effects of chemical reaction and magnetic field," *J. Heat Mass Transfer Res. (JHMTR)*, Vol. 3, No. 2, pp. 101-114 (2016).

[22] R. S. Kaluri, R. Anandalakshmi, and T. Basak, "Bejan's heatline analysis of natural convection in right-angled triangular enclosures: effects of aspect-ratio and thermal boundary conditions," *Inter. J. Therm. Sci.*, Vol. 49, No. 9, pp. 1576-1592, (2010).

[23] G. Yesiloz and O. Aydin, "Laminar natural convection in right-angled triangular enclosures heated and cooled on adjacent walls," *Inter. J. Heat Mass Transfer*, Vol. 60, pp. 365-374, (2013).

[24] H. Brinkman, "The viscosity of concentrated suspensions and solutions," *J. Chem. Phys.*, Vol. 20, No. 4, pp. 571-571, (1952).

[25] J. Maxwcll-Garnctt, "Colours in metal glasses and in metal films," *Trans. R. Soc. London*, Vol. 203, pp. 385-420, (1904).

How to cite this paper:

Ali Akbar Rashidi and Ehsan Kianpour, "Investigation of natural convection heat transfer of MHD hybrid nanofluid in a triangular enclosure,", *J. Comput. Appl. Res. Mech. Eng.*, Vol. 10, No. 2, pp. 539-549, (2021).

DOI: 10.22061/jcarme.2019.3197.1353

URL: https://jcarme.sru.ac.ir/?_action=showPDF&article=976